Competing interactions modulate the activity of Sgs1 during DNA end resection

Kristina Kasaciunaite[1], Fergus Fettes[1], Maryna Levikova[2], Peter Daldrop[3], Roopesh Anand[4], Petr Cejka[4,5], Ralf Seidel[1,3]

[1]Peter Debye Institute for Soft Matter Physics, Universität Leipzig, 04103 Leipzig, Germany

[2]Institute of Molecular Cancer Research, University of Zurich, 8057 Zurich, Switzerland

[3]Institute for Molecular Cell Biology, University of Münster, 48149 Münster, Germany
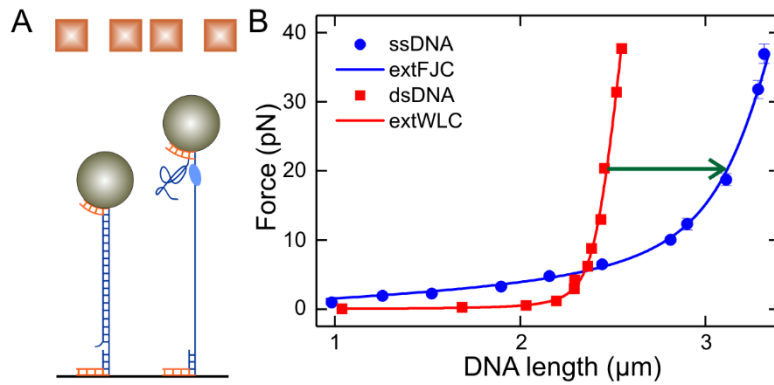
[4]Institute for Research in Biomedicine, Università della Svizzera italiana, Faculty of Biomedical Sciences, CH-6500 Bellinzona, Switzerland

[5]Department of Biology, Institute of Biochemistry, Eidgenössische Technische Hochschule (ETH) Zürich, Switzerland

Appendix

Table of contents

Fig S1 - DNA length change associated with the conversion of dsDNA to ssDNA

A   Sketch of the dsDNA construct used in this study before (left) and after full conversion to ssDNA (right). Conversion to ssDNA occurs by shearing of the flap-carrying strand either due to unwinding by a helicase or due to unzipping at forces > 65 pN. The top part of DNA is blocked in order for molecule not to anneal back to dsDNA.

B   Force-extension curves of the dsDNA construct used in this study before (red solid squares) and after (blue solid circles) conversion to ssDNA. Force extension curves were fit (solid lines) with an extensible worm-like-chain model or an extensible freely-jointed-chain model in case of dsDNA or ssDNA, respectively. The best fits provided the characteristic polymer parameters of the two DNA forms (Smith et al, 1996).The force extension data reveals that the extension of ssDNA exceeds the extension of dsDNA at forces larger than ~5 pN. DNA unwinding by a helicase (while holding the DNA at a fixed force) thus leads to a force-dependent DNA length increase (see green arrow at 20 pN in the figure). The force-extension data is used as a calibration to convert length changes at a given force into the amount of unwound DNA base pairs. The good agreement between the recorded force extension data and the fits reveals that the original molecule was dsDNA while the fully unwound molecule was mainly converted to ssDNA.
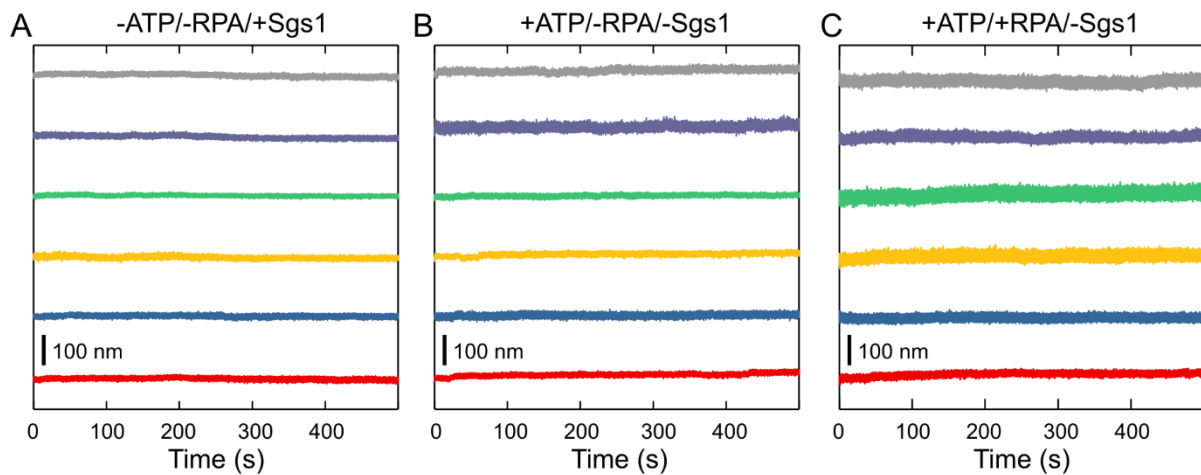
Fig S2 – ATP and Sgs1 are required to observe DNA unwinding
Absence of any detectable DNA unwinding (DNA lengthening) observed on different molecules (indicated by different colours) for the following conditions:

A   Presence of Sgs1 but absence of ATP.

B   Absence of Sgs1 but presence of ATP.

C   Absence of Sgs1 but presence of RPA and ATP.

This demonstrates that the observed DNA unwinding is due to the ATPase activity of Sgs1.
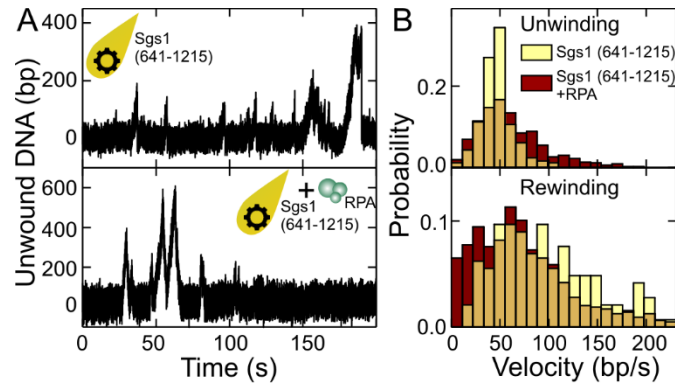
Fig S3 – DNA duplex processing by the helicase core of Sgs1 (residues 641-1215)

A   dsDNA processing patterns for the helicase core of Sgs1 in the absence (upper row) and presence of RPA (lower row). The Sgs1 helicase core shows a similar pattern as wt Sgs1 with dominant fast rezipping in the absence and slow rewinding in the presence of RPA.

B   Histograms of the observed unwinding and rewinding velocities for the helicase core of Sgs1. Noticeably, the mean unwinding velocity in the absence of RPA (47 ± 2 bp/s, $N = 674$) was considerably lower than that of wt Sgs1 (65 ± 2 bp/s). In the presence of RPA no skew of the distribution towards lower unwinding velocities was observed (a mild broadening towards higher velocities is attributed to a facilitated DNA melting in the presence of RPA). This supports that specific interactions with RPA cause the skew of the velocity distribution towards lower values for wt Sgs1. The distributions of the rewinding velocities are similar in the presence and absence of RPA though being much broader as also observed for wt Sgs1.
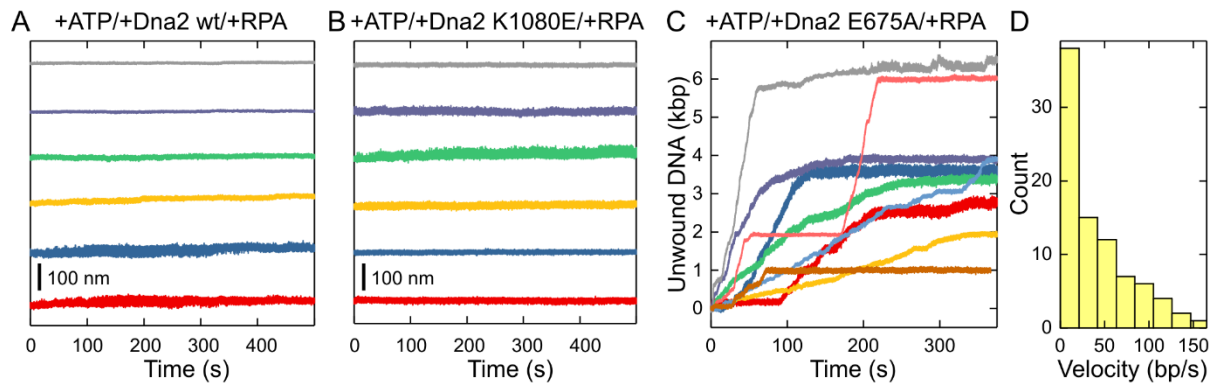
**Fig S4 – DNA unwinding by the different Dna2 variants in the presence of RPA**

A   wt Dna2 and RPA. No activity of Dna2 is observed.

B   helicase-dead Dna2 (K1080E) and RPA. No activity of Dna2 is observed.

C   nuclease-dead Dna2 (E675A) and RPA. The helicase activity of Dna2 is observed.

D   Histogram of the observed unwinding velocities for nuclease-dead Dna2.

No DNA unwinding is seen for wt and helicase-dead Dna2 since degradation of the 5' DNA flap by the active nuclease domain prevents initiation of the helicase activity. Unwinding is thus just seen for the nuclease-dead Dna2 mutant, which leaves an intact 5' flap.
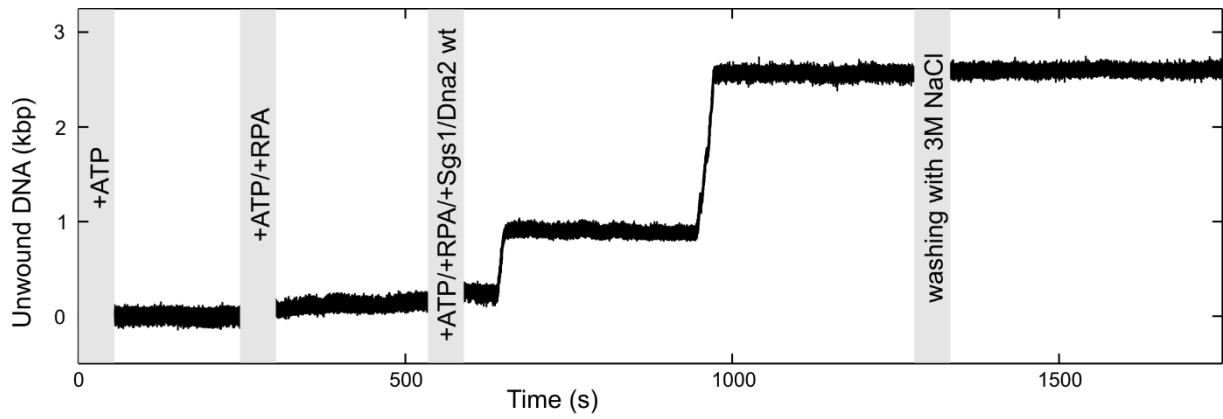
**Fig S5 – Dna2 cannot be removed from the unwinding fork**

Time trajectory of an experiment in which DNA unwinding was initiated only after the addition of Dna2 wt. After unwinding stalled, the fluidic cell was flushed twice with 300 µl of 3M NaCl (6-fold cell volume, individual flushes separated by 15 min) followed by flushing with 300 µl PBS. No detectable DNA rezipping (seen as DNA length decrease) was observed after flushing, indicating that Dna2 cannot be dissociated from the unwinding fork. The different flushing steps during which the tracking of the DNA length was stopped are indicated by gray sections that contain the added components.
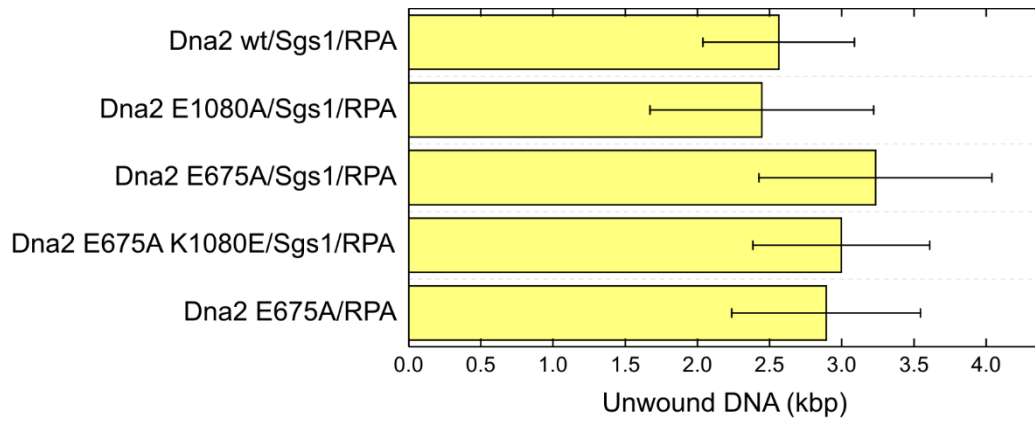
Fig S6 – Total unwound DNA by Dna2 alone or in complex with Sgs1 and RPA
The length of the unwound DNA was determined after an observation period of 30 min. Shown values represent averages of ~25 measurements. The average unwound DNA for the nuclease-dead Dna2 mutant (E675A) was within error equal to the reactions containing Sgs1 as well as wt, nuclease-dead (E675A), helicase-dead Dna2 (K1080E) or helicase-nuclease-dead Dna2 (E675A K1080E). Thus, the additional activity of Sgs1 does not provide a roadblock for Dna2.
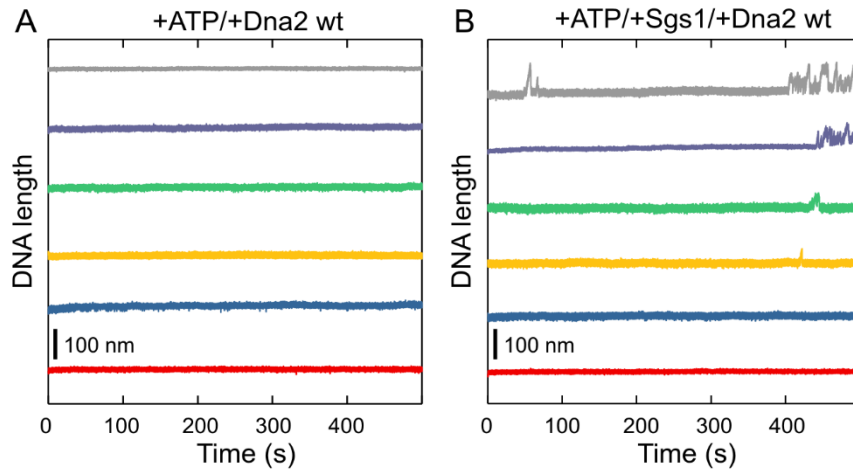
Fig S7 – Activities of Dna2 and Dna2 + Sgs1 in the absence of RPA

A   Time trajectories of the DNA length in the presence of wt Dna2 but absence of RPA. No DNA unwinding by Dna2 is observed.

B   Time trajectories of the DNA length in the presence of Sgs1 and wt Dna2 but absence of RPA. Typical saw-tooth-like unwinding patterns by Sgs1 are observed. However, no progressive DNA unwinding that would be typical for the DNA unwinding/DNA degradation by Dna2 was observed.
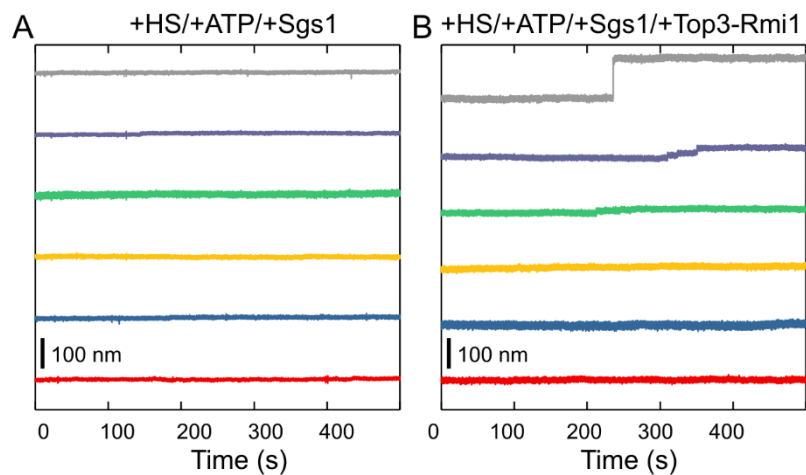
Fig S8 – Sgs1 does not unwind DNA in the absence of RPA at high salt conditions

A   Time trajectories of the DNA length in the presence of Sgs1 and ATP at high salt conditions.

B   Time trajectories of the DNA length in the presence of Sgs1, ATP and Top3-Rmi1 at high salt conditions. Gradual DNA unwinding was not observed. An occasional step-wise DNA length increase was due to the the ssDNA cleavage activity of Top3-Rmi1 (see Fig. EV3).

Note that in these experiments even a 10-fold higher Sgs1 concentration (2 nM instead of 0.2 nM Sgs1) was used in order to further stimulate the recruitment of the protein for unwinding.
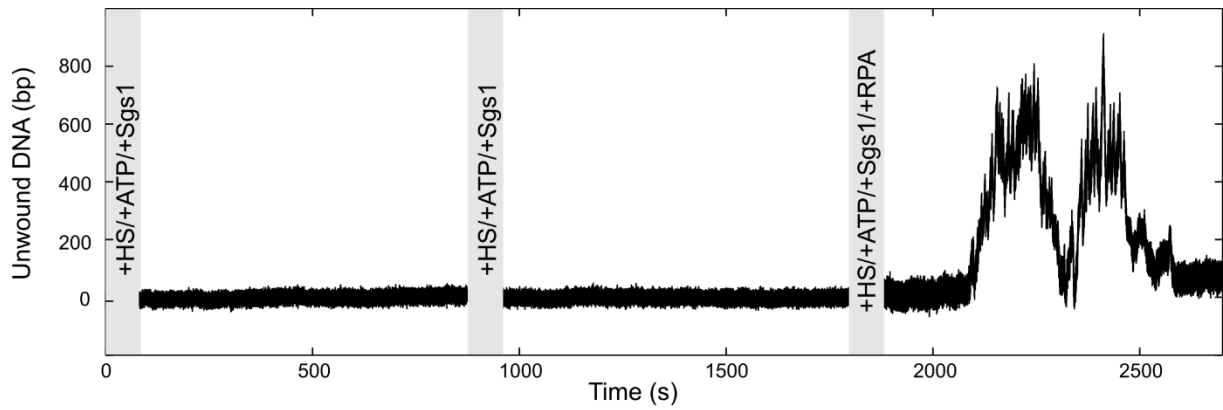
Fig S9 – RPA is required to initiate DNA unwinding by Sgs1 at high salt conditions
Time trajectory of the unwound DNA when initially adding two times Sgs1 and ATP followed by an addition of Sgs1 in the presence of RPA and ATP. Only the latter conditions provided DNA unwinding. Gray sections represent the flushing steps during which the different components were added to the fluidic cell.

Smith SB, Cui Y, Bustamante C (1996) Overstretching B-DNA: The Elastic Response of Individual Double-Stranded and Single-Stranded DNA Molecules. *Science* **271**: 795–799